Petroleum Science 23 (2026) 1675–1686

Contents lists available at ScienceDirect

Petroleum Science

journal homepage: www.keaipublishing.com/en/journals/petroleum-science

Original Paper

Possible origin of deep hydrocarbons and transformation of complex petroleum systems within the Earth's crust

Vladimir Kutcherov [a,*], Sergey Marakushev [b], Irina Plotnikova [c], Kirill Ivanov [d]

[a] KTH Royal Institute of Technology, Stockholm, 10044, Sweden
[b] Federal Research Center for Problems of Chemical Physics and Medicinal Chemistry, Moscow Region, Chernogolovka, 142432, Russia
[c] Empress Catherine II Saint Petersburg Mining University, Saint Petersburg, 199106, Russia
[d] The Zavaritsky Institute of Geology and Geochemistry, Ekaterinburg, 620016, Russia

ARTICLE INFO

Article history:
Received 19 February 2025
Received in revised form
9 June 2025
Accepted 3 November 2025
Available online 7 November 2025

Edited by Xi Zhang and Jie Hao

Keywords:
Hydrocarbon origin
Abiogenic hydrocarbons
Oil
Kerogen
Mantle
Biomarkers

ABSTRACT

We demonstrate that the conditions established in laboratory settings—such as initial reaction products, thermobaric parameters, and redox environments—are indeed analogous to those that may exist in the Earth's upper mantle. The experimental results confirmed that hydrocarbon fluids with diverse compositions can form within the upper mantle. This leads us to propose that these fluids, generated through mantle-magmatic processes, can migrate from sub-crustal zones along deep faults and fractures and be injected under high pressure into the rock, ultimately forming oil and gas deposits. As the ascending fluid cools and the partial pressure of hydrogen decreases, it transforms into liquid oil and subsequently into polymeric insoluble carbonaceous matter (kerogen) within "oil source" rocks. Our findings provide thermodynamic support for the idea that phase transitions involving CO_2, H_2O, oil, and kerogens can occur not only in the kerogen → oil but also in the oil → kerogen direction. The reversibility of phase equilibrium allows us to approach these transitions from an inorganic perspective. Consequently, we can assert that kerogen may be a product of the dehydrogenation of oil and gas. Our experimental results, which investigate the distribution of vanadyl and nickel porphyrin complexes in oils from various productive horizons, support our hypothesis that biomarkers in oils may result from the dissolution and assimilation of dispersed organic matter by ascending, high-temperature hydrocarbon fluids, rather than serving as definitive evidence of a biogenic origin.

1. Introduction

Oil and natural gas remain the primary energy sources, accounting for over 55% of the global energy balance in 2023 (Statistical Review of the World Energy, 2024). Despite more than a century of study and exploitation of hydrocarbon deposits, the origins of petroleum hydrocarbons are still subject to debate (Glasby, 2006; Kutcherov and Krayushkin, 2010; Sephton and Hazen, 2013; Wang et al., 2023). Twenty-five years ago, most (although not all) scientists would have dismissed abiogenic arguments very quickly. However, the idea did not die, and in recent years, a wide community of scientists, using a variety of methods and working independently in various parts of the world, have reopened debate regarding the possible abiogenic origin of hydrocarbons on the Earth and extra-solar planets with publications in some leading journals. Recent experimental (Kutcherov et al., 2002; Sherwood et al., 2002; Kolesnikov et al., 2009; Sonin et al., 2013; McCollom, 2016; Sokol et al., 2019; Serovaiskii and Kutcherov, 2021), theoretical (Wang et al., 2023; Zubkov et al., 1997; Karpov et al., 1998; Kenney et al., 2002; Marakushev and Marakushev, 2006a; Spanu et al., 2011; Marakushev and Belonogova, 2021), and geological data (Horita and Berndt, 1999; Charlou et al., 2002; Proskurowski et al., 2008; Marakushev and Marakushev, 2008) provide arguments to support the hypothesis of abiogenic deep origin of hydrocarbon deposits. One of the propositions suggests hydrocarbons are generated in the Earth's

* Corresponding author.
E-mail address: vladimir.kutcherov@energy.kth.se (V. Kutcherov).
Peer review under the responsibility of China University of Petroleum (Beijing).

https://doi.org/10.1016/j.petsci.2025.11.004

mantle through abiogenic (inorganic) synthesis; the resulting hydrocarbon fluid moves through the Earth's crust; it concentrates on rock formations, with their composition depending on factors such as migration rate, cooling, depth of origin, pressure, temperature, and redox conditions in the hosting rock complexes.

The goal of our work is to summarize in one text some recent results on the hypothesis of the abiogenic origin of hydrocarbons and provide arguments for its further consideration. We view our paper as a discussion and are going to focus on the following questions:

1. Can the findings from experimental studies on abiogenic synthesis of complex hydrocarbon systems under extreme thermobaric conditions, conducted in various laboratories, be extrapolated to natural environments?

The primary doubts about extrapolating the conditions established in laboratory settings to natural environments are linked to the problem of the resemblance of the redox conditions in the upper mantle to those in laboratory experiments. In this paper, we compare the redox conditions in laboratory experiments on abiogenic synthesis of hydrocarbon systems to those that may exist in the various areas of the Earth's upper mantle. The results indicate that in the upper mantle, at depths below 100 km, there are areas where the conditions are favorable for the formation of fluids containing varying amounts of CH_4 and other hydrocarbons, H_2, CO_2, and H_2O. Similar conditions were replicated in laboratory experiments. Our study shows that the conditions created in laboratory settings—such as initial reaction products, thermobaric parameters, and redox environments—are indeed similar to those that may occur in the Earth's upper mantle.

2. Can thermodynamically calculated relationships between solid, liquid, and gas phases of oil deposits and “source” rocks determine the direction of their formation process?

The thermodynamic calculations and computer simulations presented in several papers indicate that oil is generated through the progressive metamorphism of “oil source” rocks, which are the hydrocarbon sources, under increasing pressure, temperature, and burial depth. This thermodynamically reversible process is commonly understood as progressing from kerogen to oil, often referred to as the melting phase of kerogen. However, the thermodynamic data presented can be interpreted in various ways. Our paper demonstrates for the first time that the reverse process, wherein endogenous oil converts to kerogen, as the freezing phase of oil, is also a feasible possibility.

3. Are organic molecules, known as biomarkers, in oils the unambiguous sign of their biogenic origin?

Our new experimental results examining the distribution of vanadyl and nickel porphyrin complexes in oils from productive horizons of Tatarstan fields, situated at various stratigraphic levels within the sedimentary cover, support an alternative perspective. These findings suggest that the presence of biomarkers in oil may result from the dissolution and assimilation of dispersed organic matter by hot hydrocarbon fluids migrating from deeper layers to the surface.

Below, we provide a detailed discussion of the issues mentioned above.

2. Materials and methods

2.1. Methods

2.1.1. Paragenetic analysis of the C–H–O system

The paragenetic analysis presented in this study focuses on the C–H–O system and is based on the method of thermodynamic potentials. The interpretation of phase diagrams of heterogeneous systems is founded on the Gibbs phase rule, which states that the number of degrees of freedom (n) in an equilibrium thermodynamic system is determined by the number of independent components (k) plus two, minus the number of phases (F): $n = k + 2 - F$. This rule is fully applicable to the open systems being investigated, where the chemical potential or fugacity serves as the independent parameter (Korzhinsky, 1996). The equality of the chemical potential of any component in all phases governs phase equilibria in a system, and these equilibria are depicted by phase diagrams that specify the composition and ratio between the masses of equilibrium phases. The calculation of metastable facies of liquid oil, solid kerogens, and their assemblages on the temperature (T, C) – logarithm fugacity of gaseous molecular hydrogen ($\log f_{H_2}$) diagram has been carried out using thermodynamic data from reliable sources (Helgeson et al., 2009). Additionally, the free energies of the formation of gaseous alkanes at 423 K and 830 bar were calculated in the (Marakushev and Belonogova, 2021). The relationship between chemical potential and fugacity is expressed as $\mu_{H_2} = \mu 0_{H_2} + 2.303 \times RT \times \log f_{H_2}$), in which $\mu 0_{H_2}$ and f_{H_2} denote the chemical potential and fugacity of gaseous H_2 in the standard state, R is the molar gas constant (8.3145 J/mol·K), and T is the temperature in kelvins. The μ_{H_2}–T and $\log f_{O_2}$ – $\log f_{H_2}$ diagrams illustrate a system of metastable reversible equilibria, demonstrating the potential for phase transitions in one direction or another based on changes in temperature and pressure of H_2 and O_2 in the environment.

2.1.2. The separation and determination of vanadyl and nickel porphyrin complexes in oils

The process of porphyrin extraction from the oil consisted of two stages. In the first stage, 1 ± 0.2 g of crude oil was mixed with 0.5 L of ethyl alcohol and then heated in a water bath with reflux for 2 h. After being cooled (24 h), the extract was filtered through a paper filter on a Buchner funnel. Extracted alcohol with dissolved porphyrins was distilled in a vacuum. As a result, the first porphyrin concentrate was received. The oil residue and the paper filter used in the alcohol extraction were mixed with 200 mL of acetone. This mixture was heated in a water bath with reflux for 1 h and processed similarly to the alcohol extraction. As a result, the second porphyrin concentrate was received. After that, both concentrates were dissolved in benzene to a specific concentration so that the optical density of the resulting solutions was in the range of 0.4–0.8 nm. Porphyrin concentrates were transferred to graduated cylinders, and analytical spectra were recorded using a Shimadzu spectrophotometer in the visible region from 480 to 650 nm in absorption mode. The concentration of metalloporphyrins in each extract was calculated by the absorption of the long-wave α-band. The concentrations of porphyrins contained in each concentrate were summed up.

2.2. The geological settings and sample locations

2.2.1. The geological settings

The Supergiant Romashkino oil field is situated in the southeastern region of the Republic of Tatarstan, with estimated

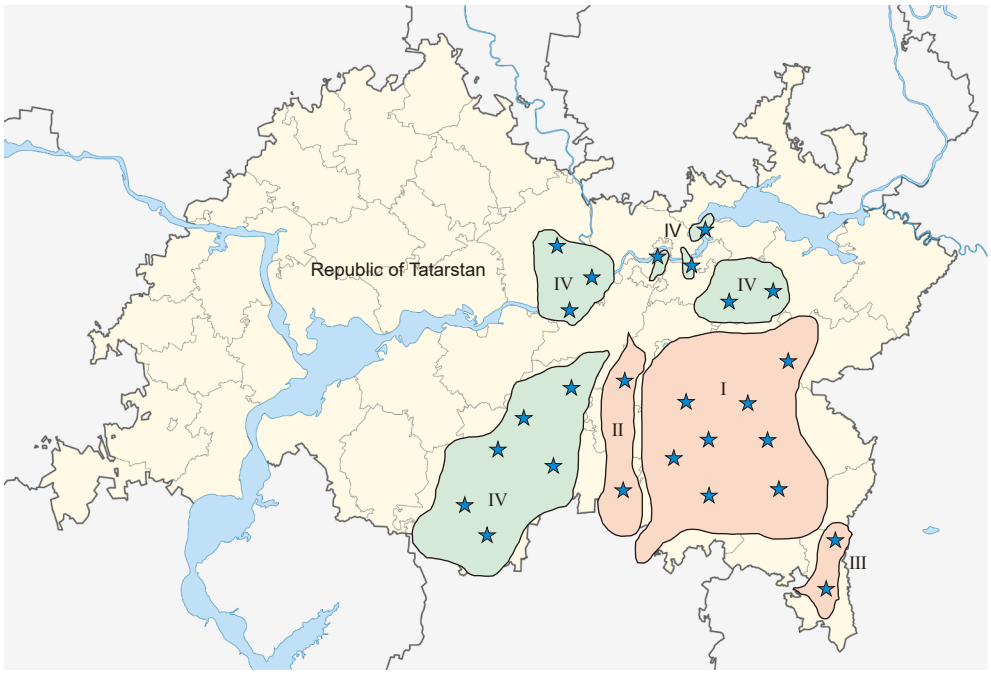

Fig. 1. Sampling sites in the Republic of Tatarstan. (I) Romashkino oil field. **(II)** Novoelkhovskoye oil field. **(III)** Bavlinskoye oil field. **(IV)** Areas of concentration of smaller fields on the slopes of the South Tatar arch. (★) Oil sampling sites.

geological oil reserves of approximately 5 billion tons (Fig. 1). This field is characterized by a typical platform-type structure, confined to a significant structural element of the second order, known as the Southern dome of the Tatar arch. This dome represents an asymmetric arched uplift, featuring uneven slopes that descend into surrounding depressions. The geological composition of the field includes Devonian, Carboniferous, and Permian deposits, with a total thickness of about 2000 m; notably, 75% of these deposits are carbonate rocks, while the remaining 25% are terrigenous. The geological framework of the area comprises two structural–geological sections: the Precambrian crystalline basement and the overlying Paleozoic sedimentary cover. The diameter of the deposit, as defined by the outer contour of the oil-bearing horizon D1, reaches between 65 and 70 km, encompassing an area of approximately 4000 km^2 (Galimov and Kamaleeva, 2015).

2.2.2. Sample locations

In our study, we analyzed the distribution of vanadyl and nickel porphyrin complexes in eighty crude oil samples obtained from 19 fields in Tatarstan, located southeast of the East European Platform (Fig. 1). These oil samples were collected from 10 productive oil and gas-bearing horizons in the sedimentary cover and then subjected to dehydration and desalting to extract the vanadium and nickel geoporphyrins.

3. Results and discussion

3.1. Evidence for abiotic deep hydrocarbon synthesis

The findings of laboratory studies conducted by various research groups provide strong evidence for the potential abiogenic synthesis of complex hydrocarbon systems at the thermobaric conditions resembling those of the Earth's upper mantle (Kolesnikov et al., 2009; Sokol et al., 2019; Kenney et al., 2002; Serovaiskii and Kutcherov, 2020; Kutcherov et al., 2010; Sonin et al., 2014; Mukhina et al., 2017; Tao et al., 2018). The reactants and thermobaric conditions in the experiments reviewed below are representative of the actual geological environment. The presence of methane, carbonates, various forms of carbon, and wustite in the upper mantle is beyond doubt (Kolesnikov et al., 2009; Shmelev and Meng, 2023; Kiseeva et al., 2022; Bataleva et al., 2015). However, several researchers have raised concerns about extrapolating the results of laboratory experiments to natural conditions (Sephton and Hazen, 2013). The primary doubts are linked to the resemblance of the redox conditions in the upper mantle to those in laboratory experiments. The redox state of the Earth's deep layers, including the lithosphere and asthenosphere, is characterized by the oxygen fugacity (f_{O_2}). The logarithmic value of (f_{O_2}) relative to the geochemical buffer FMQ (fayalite–magnetite–quartz), Δlog (FMQ), is typically used to evaluate the redox situation. This parameter governs the C–O–H composition of fluids and silicate melts and influences the stability of carbon-containing phases like diamonds, carbonates, and hydrocarbons (Taylor and Green, 1988; Ballhaus and Frost, 1994; Holloway and Blank, 1994). The heterogeneity of the redox state of the upper mantle is discussed in numerous studies (Ballhaus, 1993; Frost and McCammon, 2008). Petrological data suggest the existence of areas with low f_{O_2} values in both the lithospheric and asthenospheric layers of the upper mantle. For instance, a study of garnet peridotite xenoliths from the Kaapvaal Craton in South Africa (Luth et al., 1990; McCammon et al., 2001; Woodland and Koch, 2003), Slave Craton in Canada (McCammon and Kopylova, 2004), and Fennoscandian Shield in Finland (Woodland and Peltonen, 1999) showed that values of Δlog (FMQ) at pressures ranging from 3 to 7 GPa (corresponding to depths of 100–200 km) lie in the range of −2 to −4.5. Another study (Tychkov et al., 2008) on garnet peridotites revealed a gradual decrease in f_{O_2} to the iron-wüstite (IW) buffer (Δlog (FMQ) = −5) at a depth of 200 km. The results of studies on inclusions in natural diamonds also indicate that the mantle is characterized by reducing redox conditions, with Δlog

(FMQ) values ranging from IW to FMQ buffer (Kaminsky et al., 2015). Despite periodic redox fluctuations, the mantle becomes more reduced with increasing depth (Ballhaus and Frost, 1994; Howell et al., 2020).

The results indicate that in the upper mantle, at depths below 100 km, there are areas where the conditions are favorable for the formation of fluids containing varying amounts of CH_4 and other hydrocarbons, H_2, CO_2, and H_2O. Similar conditions were replicated in laboratory experiments, and the results are discussed below. Experiments conducted at mantle thermobaric parameters to simulate the redox environment in the upper mantle support the possibility of forming hydrocarbon systems with different compositions under these conditions. Detailed explanations of these experiments can be found in references (Sokol et al., 2019; Kolesnikov et al., 2017). Hydrocarbon formation can occur due to reactions involving carbonates, wustite, and water (Marakushev and Marakushev, 2006a; Kutcherov et al., 2010; Sonin et al., 2014; Mukhina et al., 2017) or through the hydrogenation reaction of graphite, diamond, or amorphous carbon with a hydrogen-containing fluid (Sokol et al., 2019). In studies involving the carbonate–wüstite–H_2O system under conditions like those in the upper mantle, a mixture of light alkanes, predominantly methane, was observed to form (Marakushev and Marakushev, 2006a; Kutcherov et al., 2010; Sonin et al., 2014; Mukhina et al., 2017). Furthermore, light alkanes can form even under the temperature regime of cold subduction (Mukhina et al., 2017). Modeling reactions of carbon (graphite, diamond) with a hydrogen-containing fluid under thermobaric parameters and redox conditions corresponding to the mantle environment at depths of 170–180 km revealed the formation of a mixture of hydrocarbons containing alkanes up to pentane. Increased pressure and temperature reduce methane concentration in the hydrocarbon fluid and slightly increase unsaturated and oxygen-containing hydrocarbons (Sokol et al., 2019). A study of the reaction of iron-containing dolomite (ankerite $Ca(Fe_{0.5}Mg_{0.5})CO_3)_2$ with water at a pressure of up to 6 GPa and a temperature of 1200 °C demonstrated the formation of a mixture of light alkanes up to butane (Sonin et al., 2014). Additionally, in inclusions in diamond synthesized in a metal-carbon system in the presence of a silicate substance at a pressure of 5.5 GPa and a temperature of 1500 °C, a predominance of medium (C_5–C_{12}) and heavy (C_{13}–C_{18}) aliphatic hydrocarbons was observed, indicating a highly reducing fluid in the crystallization medium (Tomilenko et al., 2021).

The findings from the study of methane at temperatures ranging from 1000 to 1500 K and pressures from 2 to 14 GPa are detailed in a paper by Kolesnikov et al. (2009). The study simulated the redox conditions of the upper mantle by introducing magnetite (Fe_3O_4) into the system, which led to the formation of a redox buffer through partial chemical transformation into iron (0). The results indicate the formation of a mixture of alkanes (methane, ethane, propane, butane) and water under the specified thermobaric conditions. The thermodynamic calculations presented in (Zubkov et al., 1997; Karpov et al., 1998; Kenney et al., 2002; Marakushev and Marakushev, 2006b) suggest that the stability of heavy and unsaturated hydrocarbons increases as pressure and temperature in the mantle rise. Experimental work by Lobanov et al. (2013) indicates that raising the thermobaric parameters to values characteristic of the lower mantle could result in the appearance of higher molecular weight alkanes in the hydrocarbon mixture. As pressures and temperatures increase, the phase composition of carbon-hydrogen fluids shifts towards heavier hydrocarbons. These experimental results demonstrate that under specific thermobaric parameters and redox conditions mimicking those of the upper mantle, stable fluids include methane, light alkanes, water, hydrogen, and oxygen-containing hydrocarbons, as indicated in (Kolesnikov et al., 2009; Sokol et al., 2019; Marakushev and Marakushev, 2006a; Kutcherov et al., 2010; Sonin et al., 2014; Kolesnikov et al., 2017). Depending on the temperature, pressure, and redox conditions, the fluid composition can vary considerably, ranging from methane-water in the upper part of the upper mantle to a fluid containing light alkanes and water at depths of 100–150 km, and a hydrocarbon-aqueous fluid enriched with heavy hydrocarbons at greater depths, as described in Kolesnikov et al. (2009, 2017); Sokol et al. (2019); Tomilenko et al. (2021).

Table 1 provides information about the experimental studies discussed in this work.

One of the possible pathways of heavier hydrocarbon formation can be described as follows. The synthesis of heavier hydrocarbons is carried out via the radical mechanism, mainly focused on the growth of the carbon–carbon bonds, isomerization, and cyclization (Fig. 2). This pathway was described in detail in Serovaiskii and Kutcherov (2020).

The result of the simulation study also shows that methane molecules fuse to form larger hydrocarbon molecules when exposed to the very high temperatures and pressures of the Earth's upper mantle (Spanu et al., 2011).

Analyzing the experimental results presented in this section allows us to answer the initial question posed in the introduction. The conditions in laboratory environments, such as the initial reaction products, thermobaric parameters, and redox environments, are comparable to those in the Earth's upper mantle. The experimental findings support the possibility of abiogenic synthesis of complex hydrocarbon systems under conditions that closely resemble the Earth's upper mantle.

3.2. Thermodynamic model of formation and phase freezing (dehydrogenation) of oil

While discussing the thermodynamic model, we employed the terms outlined by Helgeson et al. (2009).

Despite discovering several accumulations of non-methane hydrocarbons at depths of up to 10.6 km (Kutcherov and Krayushkin, 2010), the bulk of all world oil deposits is localized within the so-called “oil window” in the depth range from 3 to 5 km. In studies of followers of the biogenic concept, based on thermodynamic calculations and computer experiments to minimize the Gibbs free energy, the existence of reversible metastable phase equilibria between liquid oil, gaseous CO_2, and solid kerogens of “oil source” rocks in the physicochemical conditions of such typical oil reservoirs was substantiated (Helgeson et al., 1993; Pokrovskii and Helgeson, 1994; Richard and Helgeson, 1998; Seewald, 2001). It is postulated that oil is formed due to the progressive hydrogenation of “oil source” rocks (sources of hydrocarbons), which occurs with increasing pressure, temperature, and burial depth. An exhaustive work (Helgeson et al., 2009) shows that under *p–T* conditions of a typical oil reservoir on the shelf of the Gulf of Mexico, localized at the depths of the “oil window,” reversible equilibria are established between liquid oil, solid crystalline “mature” (low H/C ratio) and pseudo crystalline “immature” (high H/C ratio) kerogens. The phase relationships between them are interpreted as incongruent (partial) melting of solid-phase kerogen with a liquid oil phase formation. However, it is precisely this justified reversibility of reactions that allows us to consider the origin of oil deposits from the point of view of the inorganic concept, i.e., instead of the “biogenic” direction of the process kerogen → oil (phase melting), our interpretation will consider the reverse process oil → kerogen (phase freezing).

On the diagram of hydrogen pressure (in the form of the chemical potential of gaseous H_2 (μ_{H2}) – temperature (Fig. 3), we

Table 1
The experimental results confirm the possibility of the abiogenic genesis of hydrocarbon fluids under upper mantle conditions.

Reactants	Capsules	*P*, GPa	*T*, K	Analysis	Products of reaction	Reference
$CaCO_3 + FeO + H_2O$	Pt, Fe	3–5	1200–1500	GC[a], MS[b]	Alkanes up to C_6, methane predominates	Kenney et al. (2002)
$CH_4 + Fe_3O_4$	DAC	2–14	900–2500	Raman	CH_4+C_2H_6+C_3H_8+C_4H_{10}	Kolesnikov et al. (2009)
$CaCO_3 + Fe + H_2O$, graphite + $FeO + H_2O$	Pt	5	1500	GC	72%CH_4, 25%C_2H_6, 3%C_3+ 94%CH_4, 6%C_2H_6, 0.5%C_3+	Kutcherov et al. (2010)
CH_4	DAC	1.7–80	300–2000	Raman	At lower mantle conditions – a mixture of alkanes	Lobanov et al. (2013)
$CaCO_3 + FeO + H_2O$	Fe	2–6.6	550–900	GC, Raman	At T >550 K – alkanes up to C_7, benzene, methane predominates	Mukhina et al. (2017)
$Ca(Fe_{0.5}Mg_{0.5})(CO_3) + H_2O$	Au	1–6	900–1500	GC	CO_2, alkanes up to до C_4, H_2O	Tao et al. (2018)
^{13}C carbon, diamond, graphite ± H_2 ± H_2O	Pt, Au	5.5–7.8	1400–1700	GC, MS	Alkanes, oxygen-containing compounds, non-saturated hydrocarbons, H_2O	Sokol et al. (2019)
Graphite ± H_2 ± H_2O	ZrO_2	5.5	2100	GC, MS	Aliphatic (C_5H_{12}–$C_{12}H_{26}$), cyclic, oxygen-containing hydrocarbons	Tomilenko et al. (2021)

[a] Gas chromatograph.
[b] Mass spectrometer.

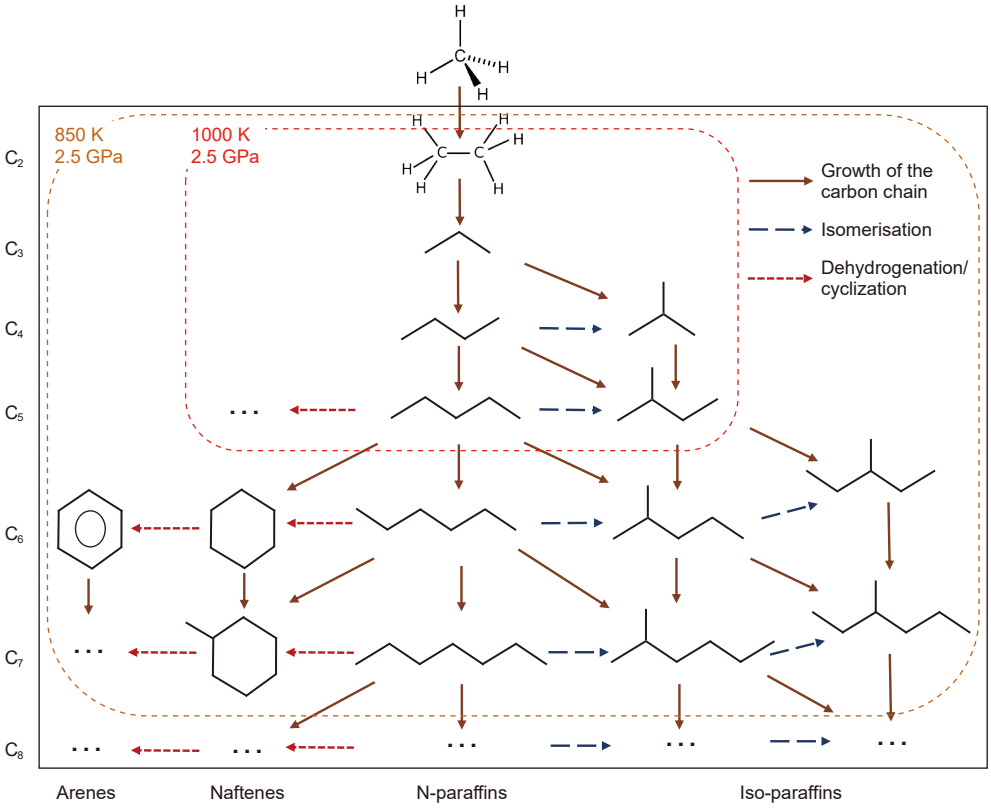

Fig. 2. Formation of heavy hydrocarbons from methane in modeled C-O-H fluid under the thermobaric conditions, corresponding to the upper mantle.

consider the relationships between phases with average equilibrium compositions, corresponding to the liquid oil ($C_{8.8}H_{16.9}$), solid "mature" ($C_{128}H_{68}O_7$ – K_2) and "immature" ($C_{292}H_{288}O_{12}$ – K_1) kerogens, as well as liquid water (H_2O) and gaseous carbon dioxide (CO_2). Hydrogen, in this system C–O–H, represented in the diagram by chemical potential, passes from extensive to intensive parameters. Then, according to the Gibbs phase rule, the two black circles in the diagram, indicated by the temperature values of 373 K and 401 K, represent invariant parageneses (assemblages) of four phases at a specific temperature, pressure, and chemical potential of the molecular hydrogen. These parageneses correspond to the stoichiometric reactions:

$$C_{292}H_{288}O_{12}\ (K_1) + 88.249H_2O = 27.486C_{8.8}H_{16.9} + 50.125CO_2 \quad (1)$$

$$C_{292}H_{288}O_{12} = 1.527C_{128}H_{68}O_7\ (K_2) + 10.899C_{8.8}H_{16.9} + 0.64CO_2 \quad (2)$$

Each invariant equilibrium is coordinated by four three-phase monovariant equilibria that separate the divariant fields (facies) of the metastable phases under consideration and their parageneses.

The diagram (Fig. 3) can be considered a thermodynamic model of an evolving inorganic oil reservoir under high carbon dioxide pressure conditions. The diagonal system of monovariant equilibria conditionally divides the diagram into two parts—the upper left corner is occupied by the facies of liquid oil of average composition $C_{8.8}H_{16.9}$, and the lower right corner is occupied by the facies of "mature" and "immature" kerogens and their parageneses. As one approaches the surface, a decrease in hydrogen

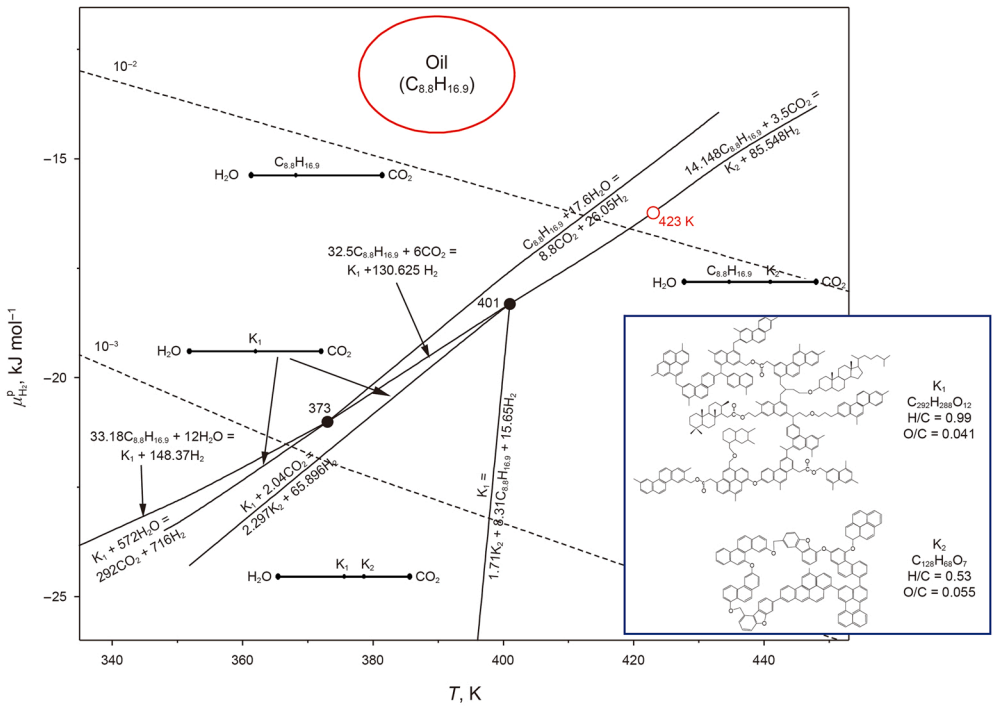

Fig. 3. Temperature—the chemical potential of gaseous hydrogen diagram. Diagram temperature (T, K)—the chemical potential of gaseous hydrogen (μ_{H_2}), depicting the reversible phase relationships among crystalline "mature" (K_2, $C_{128}H_{68}O_7$) and "immature" (K_1, $C_{292}H_{288}O_{12}$) kerogens, gaseous CO_2, liquid H_2O, and oil ($C_{8.8}H_{19.9}$). Parageneses of phases in bivariant facies are presented in line diagrams. Thermodynamic characteristics of substances are calculated according to data from (Helgeson et al., 2009). Fluid ambient pressure is determined by CO_2 fugacity ($f_{CO_2} = P_f$, where P_f corresponds to fluid pressure along the US Gulf Coast geotherm). The logarithms of the activity of liquid water, oil, and solid kerogens equal unity for pure liquid and solid matter, respectively. According to Helgeson et al. (2009), the idealized structures of kerogens are shown in the box on the right side of the diagram. Dashed lines (10^{-n}) are isobars of molecular hydrogen fugacity. The empty circle at the monovariant equilibrium indicates the redox conditions and temperature of the oil reservoir at a depth of ~4.3 km for constructing the diagram in Fig. 4.

pressure (hydrogen pressure isobars - dotted lines, Fig. 3) in the oil reservoir as a whole leads to a phase transformation of liquid oil with the formation of solid kerogens—"mature" (K_2) and "immature" (K_1). In this case, phase transitions of liquid oil through equilibria with the formation of "immature" (from 473 to 401 K) and "mature" (above 401 K) kerogens occur in overall reactions with the absorption of CO_2:

$$14.148C_{8.8}H_{16.9} + 3.5CO_2 = K_2 + 85.548H_2 \quad (3)$$

$$32.5C_{8.8}H_{16.9} + 6CO_2 = K_1 + 130.625H_2 \quad (4)$$

Below 373 K, the formation of "immature" kerogen is due to the hydration of oil, i.e., with the absorption of liquid water by oil:

$$33.18C_{8.8}H_{16.9} + 12H_2O = K_1 + 148.37H_2 \quad (5)$$

The phase transition through a high-temperature monovariant equilibrium (above 401 K), reflecting the fixation of CO_2 by oil with the formation of K_2, occurs with a decrease in the chemical potential of hydrogen and leads to the appearance of a high-temperature facies with a paragenesis of liquid oil and crystalline kerogen (reflected on the linear diagram on the right side ofFig. 3). The almost vertical equilibrium $1.71C_{128}H_{68}O_7$ (K_2) + $8.31C_{8.8}H_{16.9}$ + $15.65H_2$ = $C_{292}H_{288}O_{12}$ (K_1) separates the high-temperature facies with the K_2 kerogen-oil paragenesis and the low-temperature facies with the paragenesis: K_1 –matureK_2 kerogen. That is, it is evident that as the temperature decreases, liquid oil will transform first into "mature" and then into "immature" solid kerogens. This phase transition can be called phase freezing of liquid oil with the formation of solid kerogens in a natural process dehydrogenation reverse to experimental pyrolysis—kerogen hydrogenation reactions (Lewan, 1997; Schimmelmann et al., 2001; He et al., 2025). In general, a drop in temperature and chemical potential of hydrogen in the surrounding trace leads to phase freezing (polycondensation) of liquid oil in the process of its dehydrogenation in the overall reactions of hydration and fixation of CO_2 (introducing a third independent component into the C–H system ($C_{8.8}H_{16.9}$)– oxygen) with the formation of solid phases of kerogens of varying degrees of "maturity." Thus, oil, in relation to kerogens of different degrees of "maturity" and first to crystalline "mature" kerogen, is a kerogen-source liquid rock.

These conclusions assume that, on the geological scale of sedimentary basin formation processes, the rates of chemical reactions responsible for the formation of solid kerogen phases are higher than the rate of oil filtration through the forming shale "oil source" rocks. It should be borne in mind that the above reactions represent the sum of numerous responses, illustrating the achievement of equilibrium in a geochemical system, and do not reflect the paths and mechanisms of reactions.

Let us compare two thermodynamic systems, including liquid oil ($C_{8.8}H_{16.9}$) and crystalline "mature" kerogen ($C_{128}H_{68}O_7$), with contrasting gas phases (CO_2 and non-methane hydrocarbons (HCs) on diagrams of gaseous oxygen fugacity ($\log f_{O_2}$)–gaseous fugacity hydrogen ($\log f_{H_2}$) at a temperature of 423 K (150 °C) and a pressure of 830 bar (Figs. 3 and 4). Oxygen and hydrogen in these systems become intensive parameters, and, therefore, according to the phase rule, three-component systems C–H–O transform into single-component C-systems. In the phase space under

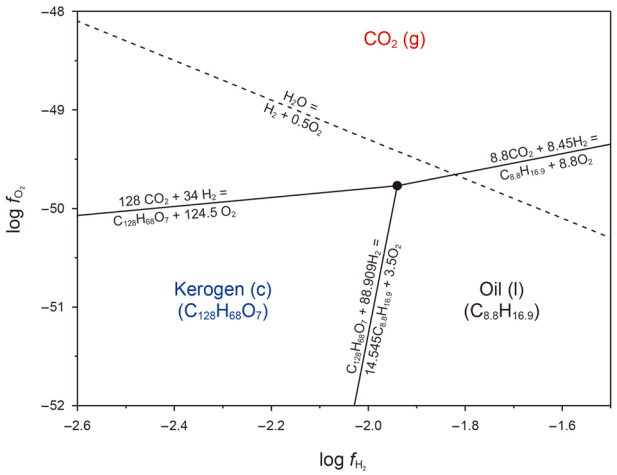

Fig. 4. Facies of liquid oil, crystalline kerogen, and gaseous carbon dioxide (CO_2). Facies of liquid oil ($C_{8.8}H_{16.9}$ (l)), crystalline kerogen ($C_{128}H_{68}O_7$ (c)), and gaseous CO_2 (g) on the phase diagram of the logarithms of fugacity gaseous H_2 ($\log f_{H_2}$) and O_2 ($\log f_{O_2}$) at a temperature of 423 K calculated according to data from (Helgeson et al., 2009) for *p–T* conditions of an oil reservoir at a depth of ~4.3 km US Gulf Coast (open red circle in the diagram, Fig. 3). The fluid pressure in the system is determined by the fugacity of CO_2 (f_{CO_2}) equal to 830 bar. The point on the diagram is the invariant three-phase equilibrium. The liquid water facies are above the saturation isopleth (dashed line). The logarithms of the activity of liquid oil and crystalline "mature" kerogen are equal to unity.

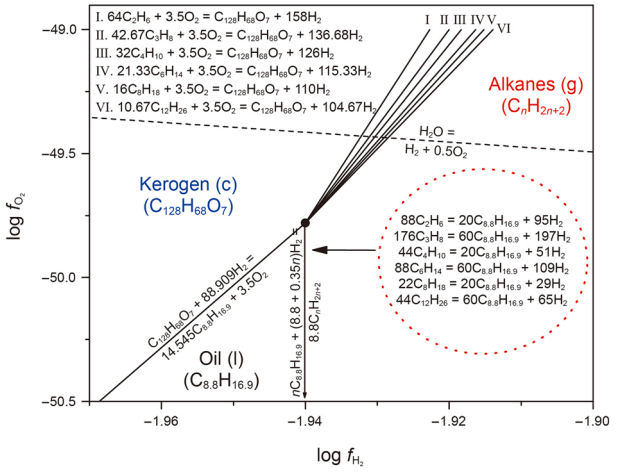

Fig. 5. Facies of liquid oil, crystalline kerogen, and gaseous hydrocarbons (alkanes). Facies of liquid oil ($C_{8.8}H_{16.9}$ (l)), crystalline kerogen ($C_{128}H_{68}O_7$ (c)), and gaseous HCs (alkanes (g)) at a pressure of 150 bar on the phase diagram of the logarithms of the fugacity of gaseous H_2 ($\log f_{H_2}$) and O_2 ($\log f_{O_2}$) at a temperature of 423 K, calculated according to (Marakushev and Belonogova, 2021; Helgeson et al., 2009). The fluid pressure in the system (830 bar) is determined by the fugacity ($f_{\sum CnHn+2}$), corresponding to the sum of the partial pressures of gas alkanes ($\sum C_nH_{n+2}$). The remaining parameters and designations correspond to the caption in Fig. 4.

consideration, the paragenesis of liquid oil and crystalline kerogen with the gas phase represents an invariant point. With that, the monovariant equilibria separate the divariant facies of these phases.

The diagram (Fig. 4) considers the equilibria between oil and "mature" kerogen and CO_2 under the redox conditions of a typical oil reservoir at high carbon dioxide pressure (Helgeson et al., 2009). A decrease in fluid pressure of hydrogen and an increase in oxygen pressure under the conditions of the Earth's surface will lead to a phase transition through monovariant equilibria with the transformation of liquid oil into "mature" crystalline kerogen and gaseous CO_2. In addition, the upward migration of oil in deep fluid flows (such as the observed oil influx into active and depleted wells at the Romashkino field in Tatarstan (Gottikh et al., 2014; Muslimov and Plotnikova, 2019)) will shift these equilibria in the same direction.

Reversible phase equilibria between oil and kerogens, shown in the diagrams (Figs. 3 and 4), are established under high CO_2 fluid pressure (830 bar) in the modern Gulf of Mexico oil field. However, the very formation of oil deposits occurred under conditions of high fluid pressure HCs (Marakushev and Marakushev, 2008, 2010); therefore, in the diagram of the logarithms of the fugacity of hydrogen ($\log f_{H_2}$) and oxygen ($\log f_{O_2}$) (Fig. 4), the gas phase is replaced by the HCs phase, as a hypothetical set of alkanes. The sum of their partial pressures equals 830 bar and determined the lithostatic pressure in the deposit. The equilibrium liquid oil-crystalline kerogen ($14.545C_{8.8}H_{16.9} + 3.5O_2 = C_{128}H_{68}O_7 + 88.909H_2$) is similar to the equilibrium presented in Fig. 3, but their relationships with the gas phase are significantly different. Vertical iso-potential monovariant stoichiometric equilibrium (with the general formula $8.8C_nH_{2n+2}$ (alkanes) $= nC_{8.8}H_{16.9}$ (oil) $+ (8.8 + 0.35n)\ H_2$), corresponding to the logarithm of hydrogen fugacity ($\log f_{H_2}$) equal to −1.94, separates metastable facies of gas alkanes and liquid oil.

The diagram (Fig. 5) shows that a decrease in hydrogen fugacity (f_{H_2}) in the forming oil reservoir should lead to a phase transition of gas alkanes with forming a liquid oil phase. With a decrease in f_{H_2}, as well as with an increase in oxygen pressure (f_{O_2}), sequential oxidation of fluid HCs (alkanes) occurs, starting with higher molecular weight ones, with the formation of crystalline "mature" kerogen. In addition, it is necessary to consider that when deep HC fluids rise to the surface, the equilibrium HCs ⟷ oil and HCs ⟷ kerogen will also shift toward the formation of oil and kerogen. In general, the phase diagram (Fig. 5) can be considered a thermodynamic model of an equilibrium petrogenic carbon reservoir (a typical oil and gas reservoir) in the form of the relationship of gas, liquid and solid phases of carbon matter at a temperature of 423 K (150 °C) and a pressure of 830 bar, as well as a physical and chemical illustration of the process of formation of oil and kerogen of "oil source" rocks from HCs when redox conditions change in the forming deposit.

Under conditions of CO_2 degassing (Fig. 4), oil can reach equilibrium with water, but "mature" kerogen cannot (the kerogen facies are below the equilibrium of water formation). In contrast, under conditions of HCs degassing (Fig. 5), "mature" kerogen can exist in paragenesis with water, but liquid oil cannot (oil facies are below the equilibrium of water formation). Therefore, according to (Helgeson et al., 2009), in the first case (Fig. 4), any water initially present (or subsequently entered) into the "oil-source" rock will irreversibly react with the "mature" kerogen to form CO_2 and/or oil. However, under conditions of HCs degassing (Fig. 5), the situation is precisely the opposite, i.e., water is a factor in the irreversibility of the phase transformation of oil into kerogen. In other words, water will react irreversibly with oil to form "mature" kerogen and/or gaseous HCs until all the water or the oil is consumed in the reactions. Thus, oil is a liquid parent rock, forming crystalline "mature" kerogen in irreversible processes under high-pressure HC fluids and in the presence of liquid H_2O. However, in the considered regimes of CO_2 or HCs degassing and without considering the influence of water as an irreversibility factor, with a geologically long-term decrease in hydrogen pressure, increase in oxygen pressure (Figs. 4 and 5), and a drop in temperature (Fig. 3) a phase transition liquid oil → crystalline kerogen, i.e., phase freezing of oil occurs.

The considered scenario for the formation of oil, gas, and polymeric carbon substances of "oil source" rocks is based on the

concept of degassing of the Fe–Ni liquid core of the Earth in the form of pulses of hydrogen fluids, which exist there in huge concentrations. The existence of a large concentration of hydrogen in the core is explained by the model of the development of the Solar System, in which the stratification of the substance of the iron-stone core of Proto-Earth (an analog of modern Jupiter) on a central liquid metal and outer solid silicate shells occurred under the enormous pressure of the hydrogen of its outer fluid envelope. As a result of the consolidation of the silicate shell and the deflation of the outer fluid hydrogen-helium shell of Proto-Earth, this massive concentration of hydrogen was preserved in the core, and its hydrogen degassing determined the further evolution of our planet (Marakushev and Marakushev, 2010). This hydrogen is a component of hydrocarbons formed due to its high-temperature and high-pressure effects on various forms of carbon (elemental carbon in multiple states of aggregation, metal carbides, and carbon oxides). The metastability of hydrocarbons at different depths of the mantle has been confirmed theoretically and in several experiments, discussed in Section 3.1. The synthesis of hydrocarbons ends the progressive stage of development of the C–H system. Then, its regressive stage begins with the formation of oil, natural gas, and the so-called "caustobiolites" (bitumen, asphaltenes, kerogens, etc.), which occurs along a gradient of decreasing hydrogen pressure and temperature in the earth's crust (Figs. 3 and 5).

The thermodynamic calculations presented in this section allow us to obtain an answer to the second question stated in the introduction. We have shown that phase transitions between reversible equilibria CO_2–oil–kerogen can occur in both the kerogen–oil direction and the oil–kerogen direction.

This interpretation suggests that kerogen can be regarded as a product of the dehydrogenation of oil and gas. One of the primary arguments put forth by advocates of the biogenic concept is the existence of specific biomarkers in oils, bitumens, kerogens, etc. The following section demonstrates that the presence of these biomarkers is attributed to the extraction of biological structures from the surrounding sedimentary rocks by the hot deep hydrocarbon fluid.

3.3. Biomarkers

The presence of biomarkers in oil can be interpreted in several ways. Specifically, these biomarkers result from the dissolution and assimilation of dispersed organic matter by hot, deep hydrocarbon fluid, a phenomenon previously confirmed through experimentation (Balitsky et al., 2023; Ivanov et al., 2010). The hydrocarbon fluid formed during mantle–magmatic processes ascends from sub-crustal zones along deep faults and fractures, permeating the basement and sedimentary strata. As this fluid comes into contact with the remains of buried biomass biochemical structures within the sedimentary cover, it extracts and carries their biological imprints while migrating through the sedimentary layers. During this migration, the deep fluid assimilates an increasing number of organic fragments from the sedimentary rocks, enriching itself with a diverse array of biomarkers. These biomarkers offer insight into the conditions under which the sediments were formed. It is also important to consider the impact of microbiological activity, which can alter the oil's composition through metabolic processes and decomposition. This influence becomes more pronounced as the depth of the deposit decreases. Consequently, the biomarker composition of oils derived from deposits formed by deep fluid migration is expected to be distinct, with the concentrations of oil biomarkers increasing as the deposits are located farther from the feeding fault.

To examine the above assumption, we studied the distribution of vanadyl and nickel porphyrin complexes in oils from productive horizons in Tatarstan fields at various sedimentary cover stratigraphic levels.

Among the well-known biomarkers are geoporphyrins (petroporphyrins)—vanadyl and nickel porphyrin complexes. Porphyrins, natural organic pigments sourced from Fe-heme proteins and Mg-chlorophyll, play a crucial role in life processes. These pigments are present in oil, meteorites, sedimentary and igneous rocks, and minerals of endogenous origin, including asphaltites, coals, peat, shales, carbonates, and deep waters. The presence of geoporphyrins in oil is generally considered an indicator of the sedimentary migration (thermogenic) origin of the entire oil composition (McKenna et al., 2021). However, porphyrins may also be extracted from host sedimentary rocks by endogenous oil, with further formation of geoporphyrins.

The chromatographic analysis of selected oil samples revealed the presence of vanadyl and nickel porphyrin complexes in all oils examined. However, the content of porphyrin complexes in oil samples from various depths varied significantly by several orders of magnitude. The minimum concentration of V-Ni-porphyrins, bordering on the precision of the method used (0.6 mg per 100 g of oil), was found in the oil from layers DIII and DIV of the Ardatovsky and Vorobievsky horizons of the Givetian stage of the Middle Devonian (Fig. 6). These layers are located at the base of the sedimentary cover close to the top of the crystalline basement. In several oil samples selected from the Vorobievsky horizon, vanadium and nickel porphyrin complexes did not exist, or their concentration was at the limit of the method's detection capability. In the Givetian stage oil, the Ni-porphyrin content ranges from 2.07 to 6.93 mg/100 g of oil, with an average of 4.2 mg/100 g, while the V-porphyrin content ranges from 5.52 to 18.3 mg/100 g of oil, averaging 8.87 mg/100 g. Meanwhile, in the oil from the Vereisky horizon of the Middle Carboniferous, the Ni-porphyrins content reaches 18.35 mg/100 g, and V-porphyrins reach 44.56 mg/100 g. Moving up the section in oils of carbonate layers from the Frasnian, Famennian, Tournaisian, Visean, and Bashkir stages, there is a noticeable increase in the amount of vanadium and nickel porphyrin complexes. Moreover, this increase occurs progressively from bottom to top. This trend is common for all studied areas of oil deposits in Tatarstan (Figs. 7 and 8).

In Fig. 9, the graph illustrates the variation in the content of V and Ni-porphyrin complexes in oils from the Vorobyovsky to Vereisky horizons in the South Tatar arch. It's worth noting that the V/Ni ratio falls within a narrow range of 2.16–2.43 despite the significant depth-based variability in productive horizons. This suggests a close genetic relationship among the oils studied and indicates a precise source for their formation.

The presence of V and Ni-porphyrin complexes in oil can be understood through the following explanation. Before the deep hydrocarbon fluids entered the sedimentary layers, these layers contained a certain quantity of porphyrin tetrapyrrole structures, likely derived from surface biological sources. Furthermore, the concentration of biological porphyrins in various horizons increased as the depth of the horizons decreased.

Hydrocarbon fluid is generated at depth as a result of alkaline magmatism. In cases where magma chambers are stratified, fluid phases with varying concentrations of ore metals, significantly exceeding the metal concentrations found in the surrounding magmas and trans magmatic fluids, are formed at different horizons. In the upper horizon of these chambers, vanadium-rich titanium-magnetite ores are formed, while the underlying critical zone yields chromite and copper-nickel ores (Marakushev and Marakushev, 2008, 2010). As hydrocarbon fluids ascend and permeate through magmatic ore melts, various metals and their

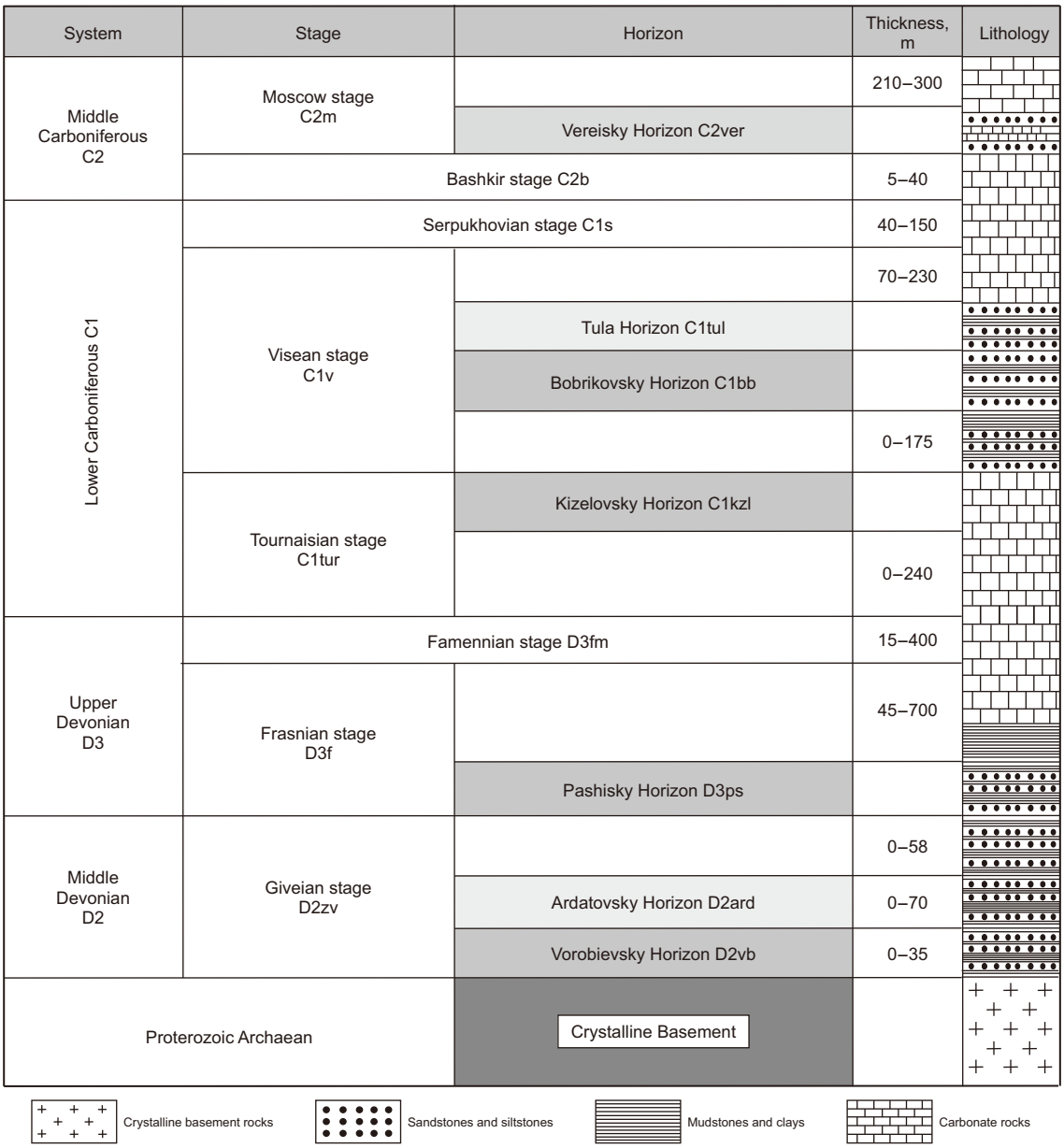

Fig. 6. Stratigraphic scheme and lithology of the sedimentary cover within the Republic of Tatarstan.

migration complexes are incorporated into the fluid composition. All types of oil exhibit abnormally high concentrations of numerous metals (V, Ni, Zn, Cu, Mo, Hg, Au, Pd, Pt), with the extraction of these metals reaching industrial significance. Among these, vanadium, nickel, and zinc are predominant, forming a distinct "oil" paragenesis. Geochemical types of oil—characterized by vanadium, nickel, or zinc—are distinguished by the predominance of one of these metals, not only in specific deposits but also across entire oil provinces (Marakushev and Marakushev, 2006b; Aleksandrova et al., 2017; Ivanov et al., 2022; Yang et al., 2023).

The deep paragenesis of V + Ni + Zn has also been identified in the bitumen extracted from diamond-bearing kimberlite pipes, which are permeable structures conducive to the migration of hydrocarbons into them. The origin of this paragenesis is linked to deep magmatic foci. Let us examine the microelement composition of the bitumen fraction found in the geodes of the Udachnaya diamond pipe located on the Siberian platform. This bitumen is characterized by asphaltite with a light ("oil") isotopic composition of carbon ($\delta^{13}C = -34.6‰$), contrasting sharply with the heavier carbon composition of the calcite present in the same location ($\delta^{13}C = +24.5‰$) (Gottikh et al., 2004).

Fig. 10 illustrates a diagram depicting the logarithms of impurity element content in asphaltite based on their ordinal numbers, highlighting their division into even and odd categories. The diagram reveals the previously discussed "oil" paragenesis of metals V + Ni + Zn (highlighted within a red dotted circle), as evidenced by the prominent maxima of their concentrations in asphaltite, which significantly surpass the levels of all other impurity elements. Notably striking is the exceptionally high concentration of vanadium, an odd element that, by the Oddo-Harkin's rule, should naturally exhibit lower prevalence compared to closely related even elements. However, the vanadium levels in asphaltite are remarkably higher than those of other impurity elements. This phenomenon can be attributed to its extraordinarily high selective chemical affinity for oxo- and sulfide complexes with

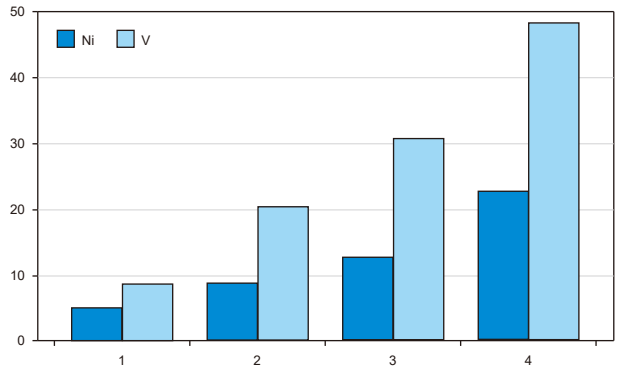

Fig. 7. Content of vanadyl (VO^{2+}) and nickel (Ni^{2+}) geoporphyrins (in mg/100 g of oil) in Zelenogradskaya area of the Romashkino oil field. (1) Vorobievsky horizon of the Givetian stage of the Middle Devonian. (2) Pashisky horizon of the lower sub-stage of the Frasnian stage of the Upper Devonian. (3) Kieselovsky horizon of the Tournaisian stage of the Lower Carboniferous. (4) Bobrikovsky horizon of the Visean stage of the Lower Carboniferous.

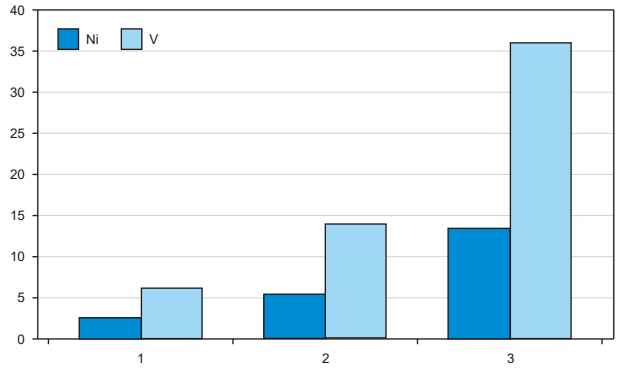

Fig. 8. Content of vanadyl (VO^{2+}) and nickel (Ni^{2+}) geoporphyrins (in mg/100 g of oil) in North Almetyevskaya area of the Romashkino oil field. (1) Ardatovsky horizon of the Givetian stage of the Middle Devonian. (2) Pashisky horizon of the lower sub-stage of the Frasnian stage of the Upper Devonian. (3) Bobrikovsky horizon of the Visean stage of the Lower Carboniferous.

hydrocarbons, which results in its effective concentration throughout the oil generation processes.

The study (Sanz-Robinson and Williams-Jones, 2020) demonstrates that liquid hydrocarbons can serve as effective ore fluids for

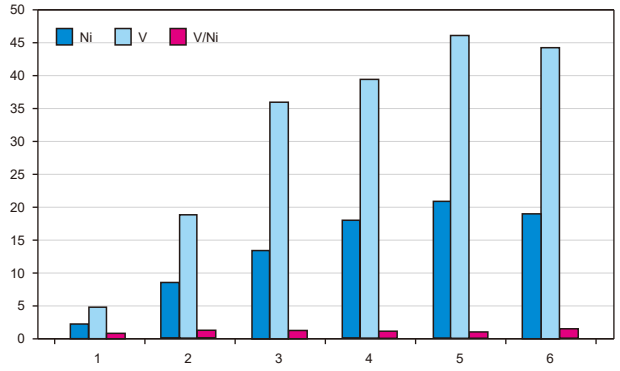

Fig. 9. Content of V, Ni-porphyrin complexes in oils of various South Tatar arch stratigraphic horizons (mg/100 g of oil). (1) Givetian stage of the Middle Devonian (Ardatovsky and Vorobievsky horizons). (2) Frasnian stage of the Upper Devonian (Pashisky horizon). (3) Tournaisian stage of the Lower Carboniferous. (4) Visean stage of the Lower Carboniferous (Bobrikovsky horizon). (5) Visean stage of the Lower Carboniferous (Tula horizon). (6) Moscow stage of the Middle Carboniferous (Vereisky horizon).

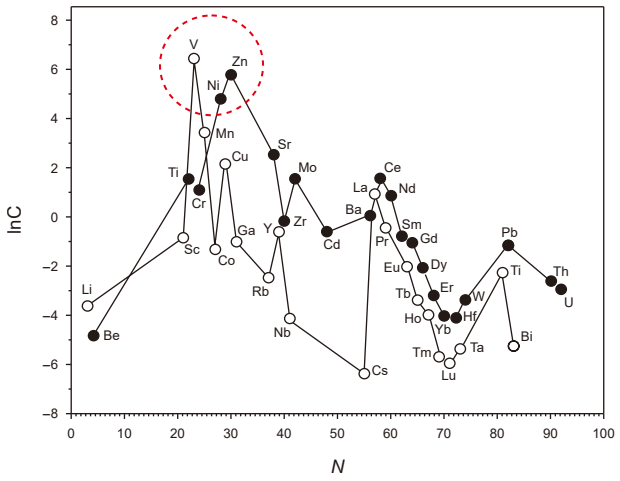

Fig. 10. The geochemical spectrum of asphaltite from the Udachnaya kimberlite pipe on the Siberian platform. *N* – the atomic numbers of elements, lnC - natural logarithms of trace element content (g/t), based on data from (Gottikh et al., 2004; Marakushev et al., 2004). The data is categorized into even (filled circles) and odd (open circles) atomic numbers. A red dotted circle highlights the V + Ni + Zn paragenesis.

nickel, with concentrations increasing alongside the sulfur content in oil due to the formation of nickel sulfide. Vanadium sulfide, specifically the greenish-black amorphous mineral patronite (VS_2), is commonly associated with nickel, iron, zinc, molybdenum, phosphorus, and carbon (Haggan and Parnel, 2000) and is characteristic of high-sulfur parent oil. Furthermore, vanadium is considered a lithophile (oxyphilic) metal, and its most stable oxidation state is the oxovanadium cation (VO^{2+}) (McKenna et al., 2021). During the deposit formation process, the VO^{2+} and Ni^{2+} cations present in the oil fluid coordinate with the tetrapyrrole ligands of porphyrins found in the surrounding sedimentary rocks. This interaction displaces magnesium and iron cations, leading to the formation of vanadium-nickel geoporphyrins. In the scenario under consideration, the deep hydrocarbon fluid that migrated into the stratigraphic horizons of the South Tatar arch along faults initially lacked porphyrin complexes but was enriched with various metals, particularly vanadium and nickel, which have origins in the deep mantle.

Our new experimental findings regarding the distribution of vanadium-nickel complexes in oils from the productive horizons of Tatarstan deposits, located at various stratigraphic levels within the sedimentary cover, along with the discussion of these results, provide us with insights to address the third question posed in the introduction.

The evidence suggests that geoporphyrins in oil may stem from the interaction between dissolved metals in ascending deep hydrocarbon fluids and biological porphyrins found within the sedimentary rocks of the examined horizons. In this context, oil, particularly from deposits in the upper horizons, appears to have a biogeochemical origin.

Therefore, deep hydrocarbon fluids, which carry specific parageneses of ore metals, contribute to the metal content of oils, thereby underscoring their deep abiogenic characteristics.

4. Conclusions

Experimental conditions for synthesizing complex hydrocarbon systems, including the initial reaction products, thermobaric parameters, and redox environments, closely replicate those found in the Earth's upper mantle. The results obtained from these

experiments provide evidence supporting the potential abiogenic synthesis of complex hydrocarbon systems under conditions analogous to those in the Earth's upper mantle. Nonetheless, the topic of deep fluid migration requires further discussion and falls outside the scope of this paper.

We have demonstrated that phase transitions between reversible equilibria of kerogen and oil can occur in both the kerogen-to-oil and oil-to-kerogen directions. This interpretation implies that kerogen can be viewed as a product of the dehydrogenation of oil and gas.

Our new experimental results indicate that geoporphyrins in oil may arise from the interaction between dissolved metals in ascending deep hydrocarbon fluids and biological porphyrins present within the sedimentary rocks of the studied horizons.

The arguments presented in the paper support the concept of the deep abiogenic origin of hydrocarbons and provide insights into the formation of oil deposits. However, there are still several outstanding questions:

(1) Can lithological traps harbor hydrocarbon deposits at depths exceeding 11 km?

This is a pivotal question for determining the exploratory depth of ultra-deep drilling and identifying suitable drilling locations.

(2) Can the process of oil dehydrogenation, leading to various types of kerogen formation, be experimentally simulated? New experimental data will enhance our understanding of the pathways and molecular mechanisms involved in forming different oil types and their degradation products during the regressive dehydrogenation of hydrocarbon fluids rising to the Earth's surface.
(3) How will embracing the concept of the abiogenic deep origin of hydrocarbons impact our outlook on the prospects for oil and natural gas production in the medium and long term?

This concept prompts a re-evaluation of the structure, extent, and geographical distribution of the world's hydrocarbon resources, guiding future exploration endeavors.

CRediT authorship contribution statement

Vladimir Kutcherov: Validation, Writing – original draft, Conceptualization, Writing – review & editing, Investigation, Methodology. **Sergey Marakushev:** Methodology, Writing – original draft, Investigation. **Irina Plotnikova:** Writing – original draft, Investigation, Methodology. **Kirill Ivanov:** Validation, Writing – original draft.

Data availability statement

The data presented in this study are available on request from the corresponding author.

Funding

This research received no external funding.

Declaration of competing interest

The authors declare no conflicts of interest.

Acknowledgement

The article corresponds to the scientific directions ‘Study of thermodynamic processes of the Earth from the standpoint of the genesis of hydrocarbons at great depths’ (project FSRW-2024-0008) and ‘Investigation of biomimetic catalysis in autocatalytic networks of carbon dioxide fixation and redox transformation of hydrocarbons’ (project FFSG-2024-0004, registration number 124020200104-8).

References

Aleksandrova, T., Aleksandrov, A., Nikolaeva, N., 2017. An investigation of the possibility of extraction of metals from heavy oil. Miner. Process. Extr. Metall. Rev. 38 (2), 92–95. https://doi.org/10.1080/08827508.2016.1262860.

Balitsky, V.S., Setkova, T.V., Balitskaya, L.V., Golunova, M.A., Bublikova, T.M., Plotnikova, I.N., Aranovich, L.Ya., 2023. Hetero- and homogeneous states of hydrocarbon fluids in the earth's interior: Evidence from the study of synthetic fluid inclusions. Dokl. Earth Sci. 509, 133–138. https://doi.org/10.31857/S2686739722602617.

Ballhaus, C., 1993. Redox states of lithospheric and asthenospheric upper mantle. Contrib. Mineral. Petrol. 114, 331–348. https://doi.org/10.1007/BF01046536.

Ballhaus, C., Frost, B.R., 1994. The generation of oxidized CO_2-bearing basaltic melts from reduced CH_4-bearing upper mantle sources. Geochem. Cosmochim. Acta 58, 4431–4440.

Bataleva, Y., Palyanov, Y., Borzdov, Y., Bayukov, O., Sobolev, N., 2015. Conditions for diamond and graphite formation from iron carbide at the *P-T* parameters of lithospheric mantle. Russ. Geol. Geophys. 57 (1), 176–189. https://doi.org/10.1016/j.rgg.2016.01.012.

Charlou, J.-L., Donval, J.P., Fouquet, Y., Jean-Baptiste, P., 2002. Geochemistry of high H_2 and CH_4 vent fluids issuing from ultramafic rocks at the Rainbow hydrothermal field (36°14′N, MAR). Chem. Geol. 191, 345–359. https://doi.org/10.1016/S0009-2541(02)00134-1.

Frost, D.J., McCammon, C.A., 2008. The redox state of Earth's mantle. Annu. Rev. Earth Planet Sci. 36, 389–420. https://doi.org/10.1146/annurev.earth.36.031207.124322.

Galimov, E.M., Kamaleeva, A.I., 2015. Source of hydrocarbons in the supergiant Romashkino oilfield (Tatarstan): Recharge from the crystalline basement or source sediments? Geochem. Int. 53 (2), 95–112. https://doi.org/10.1134/S0016702915020032.

Glasby, G.P., 2006. Abiogenic origin of hydrocarbons: An historical overview. Resour. Geol. 56 (1), 83–96. https://doi.org/10.1111/j.1751-3928.2006.tb00271.x.

Gottikh, R.P., Pisotskiy, B.I., Plotnikova, I.N., 2014. Reduced fluids in the crystalline basement and the sedimentary basin (on an example of Romashkino and Verkhne-Chonskoye oil fields. ARPN J. Earth Sci. 3 (1), 25–41. https://doi.org/10.1016/j.gexplo.2008.11.041.

Gottikh, R.P., Pisotskii, B.I., Zhuravlev, D.Z., 2004. Trace element distribution in the kimberlite-bitumen and basalt-bitumen systems in diatremes of the Siberian Craton. Dokl. Earth Sci. 399, 1222–1226.

Haggan, T., Parnel, J., 2000. Hydrocarbon–metal associations in the Western Cordillera, Central Peru. J. Geochem. Explor. 69 (70), 229–234. https://doi.org/10.1016/S0375-6742(00)00013-3.

He, K., Wang, X.M., Yang, C.L., Xie, L.F., Zhang, S.C., 2025. C/H isotope fractionation of hydrocarbon gases from hydrogenation of organic matter: Insights from hydrothermal experiments. Org. Geochem. 199, 104884. https://doi.org/10.1016/j.orggeochem.2024.104884.

Helgeson, H.C., Richard, L., McKenzie, W.F., Norton, D.L., Schmitt, A., 2009. A chemical and thermodynamic model of oil generation in hydrocarbon source rocks. Geochem. Cosmochim. Acta 73 (3), 594–695. https://doi.org/10.1016/j.gca.2008.03.004.

Helgeson, H.C., Knox, A.M., Owens, C.E., Shock, E.L., 1993. Petroleum, oil field waters, and authigenic mineral assemblages: Are they in metastable equilibrium in hydrocarbon reservoirs? Geochem. Cosmochim. Acta 57, 3295–3339. https://doi.org/10.1016/0016-7037(93)90541-4.

Holloway, J.R., Blank, J.G., 1994. Application of experimental results to C-O-H species in natural melts. Rev. Mineral. 30, 187–230.

Horita, J., Berndt, M.E., 1999. Abiogenic methane formation and isotopic fractionation under hydrothermal condition. Science 285, 1055–1057. https://doi.org/10.1126/science.285.5430.1055.

Howell, D., Stachel, T., Stern, R., et al., 2020. Deep carbon through time: Earth's diamond record and its implications for carbon cycling and fluid speciation in the mantle. Geochem. Cosmochim. Acta 275, 99–112. https://doi.org/10.1016/j.gca.2020.02.011.

Ivanov, K.S., Fedorov, Y.N., Petrov, L.A., Shishmakov, A.B., 2010. The nature of biomarkers in oils. Dokl. Earth Sci. 432 (1), 626–630.

Ivanov, K.S., Erokhin, Y.V., Kudryavtsev, D.A., 2022. Inorganic geochemistry of crude oils of northern Eurasia after ICP-MS data as clear evidence for their deep origin. Energies 15 (1), 48. https://doi.org/10.3390/en15010048.

Kaminsky, F.V., Ryabchikov, I.D., Wirth, R., 2015. A primary natrocarbonatitic association in the Deep Earth. Mineral. Petrol. 109. https://doi.org/10.1007/s00710-015-0368-4.
Karpov, I.K., Zubkov, V.S., Bychinsky, V.A., et al., 1998. Detonation of heavy hydrocarbons in mantle flows. Geol. Geophys. 39 (6), 754–762.
Kenney, J.F., Kutcherov, V.A., Bendeliani, N.A., Alekseev, V.A., 2002. The evolution of multicomponent systems at high pressures: VI. The thermodynamic stability of the hydrogen-carbon system: The genesis of hydrocarbons and the origin of petroleum. Proc. Natl. Acad. Sci. USA 99, 10976–10981. https://doi.org/10.1073/pnas.172376899.
Kiseeva, E.S., Korolev, N., Koemets, I., et al., 2022. Subduction-related oxidation of the sublithospheric mantle evidenced by ferropericlase and magnesiowüstite diamond inclusions. Nat. Commun. 13, 7517. https://doi.org/10.1038/s41467-022-35110-x.
Kolesnikov, A., Kutcherov, V.G., Goncharov, A.F., 2009. Methane-derived hydrocarbons produced under upper-mantle conditions. Nat. Geosci. 2, 566–570. https://doi.org/10.1038/ngeo591.
Kolesnikov, A.Y., Saul, J.M., Kutcherov, V.G., 2017. Chemistry of hydrocarbons under extreme thermobaric conditions. ChemistrySelect 2, 1336–1352. https://doi.org/10.1002/slct.201601123.
Korzhinsky, D.S., 1966. On thermodynamics of open systems and phase rule. Geochem. Cosmochim. Acta 30 (8), 829–836. https://doi.org/10.1016/0016-7037(66)90135-9.
Kutcherov, V.G., Bendeliani, N.A., Alekseev, V.A., Kenney, J.F., 2002. Synthesis of hydrocarbons from minerals at pressures up to 5 GPa. Dokl. Phys. Chem. 387, 328–330. https://doi.org/10.1023/A:1021758915693.
Kutcherov, V.G., Krayushkin, V.A., 2010. Deep-seated abiogenic origin of petroleum: from geological assessment to physical theory. Rev. Geophys. 48, 1–30. https://doi.org/10.1029/2008RG000270.
Kutcherov, V.G., Kolesnikov, A., Dyugheva, T.I., Kulikova, L.F., Nikolaev, N.N., Sazanova, O.A., Braghkin, V.V., 2010. Synthesis of complex hydrocarbon systems at temperatures and pressures corresponding to the Earth's upper mantle conditions. Dokl. Phys. Chem. 433, 132–135. https://doi.org/10.1134/S0012501610070079.
Lewan, M.D., 1997. Experiments on the role of water in petroleum formation. Geochimica et Cosmochimica Acta 61, 3691–3723. https://doi.org/10.1016/S0016-7037(97)00176-2, 1997.
Lobanov, S.S., Chen, P.N., Chen, X.J., Zha, C.S., Litasov, K.D., Mao, H.K., Goncharov, A.F., 2013. Carbon precipitation from heavy hydrocarbon fluid in deep planetary interiors. Nat. Commun. 4, 2446. https://doi.org/10.1038/ncomms3446.
Luth, R.W., Virgo, D., Boyd, F.R., Wood, B.J., 1990. Ferric iron in mantle-derived garnets. Contrib. Mineral. Petrol. 104, 56–72. https://doi.org/10.1007/BF00310646.
Marakushev, A.A., Pisotskii, B.I., Paneyakh, N.A., Gottikh, R.P., 2004. Geochemical features of oil and the origin of oil fields. Dokl. Earth Sci. 399, 1120–1124.
Marakushev, A.A., Marakushev, S.A., 2006a. PT facies of elementary, hydrocarbon, and organic substances in the C-H-O system. Dokl. Earth Sci. 406 (1), 141–147. https://doi.org/10.1134/S1028334X0601034X.
Marakushev, A.A., Marakushev, S.A., 2006b. Nature of specific geochemical features of oil. Dokl. Earth Sci. 411 (8), 1303–1308. https://doi.org/10.1134/S1028334X06080319.
Marakushev, A.A., Marakushev, S.A., 2008. Formation of oil and gas fields. Lithol. Miner. Resour. 43, 454–469. https://doi.org/10.1134/S0024490208050039.
Marakushev, A.A., Marakushev, S.A., 2010. Fluid evolution of the Earth and origin of the biosphere. In: Florinsky, I.V. (Ed.), Man and the Geosphere. Nova Science Publishers Inc., New York, U.S.A., pp. 3–31. https://doi.org/10.13140/2.1.4787.9363
Marakushev, S.A., Belonogova, O.V., 2021. An inorganic origin of the “oil-source” rocks carbon substance. Georesursy 23 (3), 164–176. https://doi.org/10.18599/grs.2021.3.19.
McCollom, T.M., 2016. Abiotic methane formation during experimental serpentinization of olivine. Proc. Natl. Acad. Sci. USA 113 (49), 13965–13970. https://doi.org/10.1073/pnas.1611843113.
McCammon, C.A., Griffin, W.L., Shee, S.R., O'Neill, H. St.C., 2001. Oxidation during metasomatism in ultramafic xenoliths from the Wesselton kimberlite, South Africa: implications for the survival of diamond. Contrib. Mineral. Petrol. 141, 287–296. https://doi.org/10.1007/s004100100244.
McCammon, C., Kopylova, M.G., 2004. A redox profile of the Slave mantle and oxygen fugacity control in the cratonic mantle. Contrib. Mineral. Petrol. 148, 55–68. https://doi.org/10.1007/s00410-004-0583-1.
McKenna, A.M., Chacón-Patiño, M.L., Vallverdu, G.S., Bouyssiere, B., Giusti, P., Afonso, C., Shi, Q., Combariza, M.Y., 2021. Advances and challenges in the molecular characterization of petroporphyrins. Energy Fuel. 35 (22), 18056–18077. https://doi.org/10.1021/acs.energyfuels.1c02002.
Mukhina, E., Kolesnikov, A., Kutcherov, V., 2017. The lower *p-T* limit of deep hydrocarbon synthesis by $CaCO_3$ aqueous reduction. Sci. Rep. 7, 5749. https://doi.org/10.1038/s41598-017-06155-6.
Muslimov, R.Kh., Plotnikova, I.N., 2019. Replenishment of oil deposits from the position of a new concept of oil and gas formation. Georesources 21 (4), 40–48. https://doi.org/10.18599/grs.2019.4.40-48.
Pokrovskii, V.A., Helgeson, H.C., 1994. Solubility of petroleum in oil-field waters as a function of the oxidation state of the system. Geology 22 (9), 851–854. https://doi.org/10.1130/0091-7613(1994)022<0851:SOPIOF>2.3.CO,2.
Proskurowski, G., Lilley, M.D., Seewald, J.S., Früh-Green, G.L., Olson, E.J., Lupton, J.E., Sylva, S.P., Kelley, D.S., 2008. Abiogenic hydrocarbon production at lost city hydrothermal field. Science 319, 604–607. https://doi.org/10.1126/science.1151194.
Richard, L., Helgeson, H.C., 1998. Calculation of the thermodynamic properties at elevated temperatures and pressures of saturated and aromatic high molecular weight solid and liquid hydrocarbons in kerogen, bitumen, petroleum, and other organic matter of biogeochemical interest. Geochimica et Cosmochimica Acta 62, 3591–3636. https://doi.org/10.1016/S0016-7037(97)00345-1.
Sanz-Robinson, J., Williams-Jones, A.E., 2020. The solubility of Nickel (Ni) in crude oil at 150, 200, and 250 °C and its application to ore genesis. Chem. Geol. 533, 119443. https://doi.org/10.1016/j.chemgeo.2019.119443.
Schimmelmann, A., Boudou, J.P., Lewan, M.D., Wintsch, R.P., 2001. Experimental controls on D/H and $^{13}C/^{12}C$ ratios of kerogen, bitumen and oil during hydrous pyrolysis. Org. Geochem. 32, 1009–1018. https://doi.org/10.1016/S0146-6380(01)00059-6.
Seewald, J.S., 2001. Aqueous geochemistry of low molecular weight hydrocarbons at elevated temperature and pressure: Constrains from mineral buffered laboratory experiments. Geochimica et Cosmochimica Acta 65, 1641–1664. https://doi.org/10.1016/S0016-7037(01)00544-0.
Sephton, M.A., Hazen, R.M., 2013. On the origins of deep hydrocarbons. Rev. Mineral. Geochem. 75 (1), 449–465. https://doi.org/10.2138/rmg.2013.75.14.
Serovaiskii, A., Kutcherov, V., 2020. Formation of complex hydrocarbon systems from methane at the upper mantle thermobaric conditions. Sci. Rep. 10, 4559. https://doi.org/10.1038/s41598-020-61644-5.
Serovaiskii, A., Kutcherov, V., 2021. The role of iron carbide in the abyssal formation of hydrocarbons in the upper mantle. Geosciences 11, 163. https://doi.org/10.3390/geosciences11040163.
Sherwood, Lollar B., Westgate, T.D., Ward, J.A., Slater, G.F., Lacrampe-Couloume, G., 2002. Abiogenic formation of alkanes in the Earth's crust as a minor source for global hydrocarbon reservoirs. Nature 416 (6880), 522–524. https://doi.org/10.1038/416522a.
Shmelev, V.R., Meng, F.C., 2023. Evidence of ultrahigh-pressure evolution of garnet peridotites in the polar urals. Dokl. Earth Sci. 513, 1167–1172. https://doi.org/10.1134/S1028334X2360175X.
Sokol, A.G., Tomilenko, A.A., Bul'bak, T.A., Sokol, I.A., Zaikin, P.A., Palyanova, G.A., Palyanov, Y.N., 2019. Hydrogenation of carbon at 5.5–7.8 GPa and 1100–1400 °C: Implications to formation of hydrocarbons in reduced mantles of terrestrial planets. Phys. Earth Planet. Inter. 291, 12–23. https://doi.org/10.1016/j.pepi.2019.04.002.
Sonin, V.M., Chepurov, A.I., Zhimulev, E.I., Chepurov, A.A., Sobolev, N.V., 2013. Surface graphitization of diamond in K_2CO_3 melt at high pressure. Dokl. Earth Sci. 451, 858–860. https://doi.org/10.1134/S1028334X13080126.
Sonin, V.M., Bul'bak, T.A., Zhimulev, E.I., Tomilenko, A.A., Chepurov, A.I., Pokhilenko, N.P., 2014. Synthesis of heavy hydrocarbons under P-T conditions of the Earth's upper mantle. Dokl. Earth Sci. 454, 32–36. https://doi.org/10.1134/s1028334x1401005x.
Spanu, L., Donadio, D., Hohl, Schwegler, E., Galli, G., 2011. Stability of hydrocarbons at deep Earth pressures and temperatures. Proc. Natl. Acad. Sci. USA 108 (17), 6843–6846. https://doi.org/10.1073/pnas.1014804108.
Statistical Review of the World Energy. 2024, 73 edition. Available online: file:///C:/Users/vku/Downloads/Statistical%20Review%20of%20World%20Energy%20(1).pdf(accessed on 6.October.2025).
Tao, R., Zhang, L., Tian, M., Zhu, J., Liu, X., Liu, J., Höfer, H.E., Stagno, V., Fei, V., 2018. Formation of abiotic hydrocarbon from reduction of carbonate in subduction zones: Constraints from petrological observation and experimental simulation. Geochim et Cosmochim Acta 239, 390–408. https://doi.org/10.1016/j.gca.2018.08.008.
Taylor, W.R., Green, D.H., 1988. Measurement of reduced peridotite-C-O-H solidus and implications for redox melting of the mantle. Nature 332 (6162), 349–352. https://doi.org/10.1038/332349a0.
Tomilenko, A.A., Chepurov, A.A., Sonin, V.M., et al., 2021. Composition of volatiles captured by diamonds during growth in the metal–carbon–silicate system at high pressure and high temperature. Geochem. Int. 59, 840–850. https://doi.org/10.1134/S0016702921080085.
Tychkov, N.S., Pokhilenko, N.P., Kuligin, S.S., Malygina, E.V., 2008. Composition and origin of peculiar pyropes from lherzolites: Evidence for the evolution of the lithospheric mantle of the Siberian platform. Russ. Geol. Geophys. 49 (4), 225–239. https://doi.org/10.1016/j.rgg.2007.11.009.
Wang, C., Tao, R., Walters, J.B., Ren, T., Nan, J., Zhang, L., 2023. Deciphering the origin of abiotic organic compounds on Earth: Review and future prospects. Acta Geol. Sin. 97 (1), 288–308. https://doi.org/10.1111/1755-6724.15045.
Woodland, A.B., Peltonen, P. Ferric iron contents of garnet and clinopyroxene and estimated oxygen fugacities of peridotite xenoliths from the Eastern Finland Kimberlite Province. https://doi.org/10.29173/ikc2947.
Woodland, A.B., Koch, M., 2003. Variation in oxygen fugacity with depth in the upper mantle beneath Kaapvaal Craton, South Africa. Earth Planet Sci. Lett. 214, 295–310. https://doi.org/10.1016/S0012-821X(03)00379-0.
Yang, W., Casey, J.F., Gao, Y., Bissada, K.K., Curiale, J.A., Liao, Z., 2023. Trace elements and organic geochemical fingerprinting of natural crude oils from the Monterey Formation, offshore Santa Maria Basin, California. Mar. Petrol. Geol. 157, 106472. https://doi.org/10.1016/j.marpetgeo.2023.106472.
Zubkov, V.S., Karpov, I.K., Bychinskii, V.A., Stepanov, A.N., 1997. Thermodynamic model for the C-H system under elevated temperatures and pressures. Geochem. Int. 36, 85–90.